



## Regular article

## Single-longitudinal-mode generation in a Ho: YLF ring laser with double corner cubes resonator

Jing Wu, Yunpeng Wang, Tongyu Dai, Youlun Ju\*, Baoquan Yao, Yuezhu Wang

National Key Laboratory of Tunable Laser Technology, Harbin Institute of Technology, Harbin 150001, China

## ARTICLE INFO

## Keywords:

Tunable  
Single-longitudinal-mode  
Ho:YLF ring laser  
Double corner cubes

## ABSTRACT

In this paper, output characteristics of single-longitudinal-mode Ho: YLF ring laser are firstly investigated in double corner cubes configuration. Single-longitudinal-mode laser output is realized by a faraday rotator and a half-wave plate, and an F-P etalon is inserted into the cavity to realize wavelength tuning. The principle of unidirectional operation of the Ho: YLF ring laser with double corner cubes is firstly analyzed with the method of optic matrix and transition matrix. A highest single-longitudinal-mode power of 733 mW at 2065.68 nm is achieved and the slope efficiency is 12%. The tunable range is about 238 GHz and  $M^2$  factor is 1.21. The results show that the single-longitudinal-mode Ho: YLF ring cavity with double corner cubes is a potential way to improve the misalignment sensitivity.

## 1. Introduction

2  $\mu\text{m}$  solid state lasers operating in the eye-safe waveband have many important applications [1–5], including high-resolution spectroscopy [6], medicine, laser remote sensing, laser lidar or wavelength conversion to 3–12  $\mu\text{m}$  [7–8]. In many military applications, 2  $\mu\text{m}$  single-longitudinal-mode (SLM) lasers with stable operation, anti-interference ability and small volume are urgently required. Especially for 2  $\mu\text{m}$  differential absorption lidar (DIAL) for atmospheric  $\text{H}_2\text{O}$  and  $\text{CO}_2$  monitoring [9–16], tunable seed laser with high power, and high misalignment sensitivity can improve the locking probability of the injection locked laser. In 2017, our group reported a tunable SLM Ho: YLF ring laser based on Faraday effect [17]. Output power at 2051.65 nm achieved 528 mW with four-mirror bow-tie ring cavity structure. Highest power of 1.5 W was obtained by master oscillator power amplifier technique. In order to further enhance the misalignment sensitivity of the SLM Ho: YLF ring laser, corner cube prism is used as resonator mirrors on account of the reflection characteristic of spatial orientation [18–19]. A mass of investigations on solid-state lasers with single corner cube have been tried to improve the anti-misalignment sensitivity. In 2000, Wu et al. demonstrated a corner cube laser based on a Nd: YAG crystal [20]. A nonplanar ring oscillator was used to generate 100 mW single-frequency operation. In 2010, Ma et al. reported a pulsed Ce: Nd: YAG laser with a corner cube and  $\text{Cr}^{4+}$ : YAG was used as a Q-switching element [21]. The results show that the laser has excellent average pulse energy stability and divergence angle stability under varied environment temperature. In 2013, Cheng et al.

reported a six Nd: YAG solid state laser coherent combination with a corner cube [22]. Combining output energy of 15.3 J was obtained with the combining efficiency of 95.6%. In 2016, our group reported a SLM Ho: YAG laser with a corner cube cavity [23]. Up to 478 mW SLM power was obtained by the method of intracavity etalons and the slope efficiency was 7.9%. As we know, this is the first report on 2.06  $\mu\text{m}$  SLM Ho: YLF ring laser with double corner cubes.

In this letter, we demonstrate a novel SLM Ho: YLF ring laser with double corner cubes. The ring laser with double corner cube has the advantage of high anti-misalignment sensitivity and small volume. Ho: YLF crystal is more suitable for the cavity with double corner cubes than isotropic crystals for its birefringence property [24–27]. The principle of unidirectional operation of the Ho: YLF ring laser with double corner cubes is firstly analyzed with the method of optic matrix and transition matrix. The highest SLM power of 733 mW at 2065.68 nm is obtained by eliminating the spatial hole-burning effect and the slope efficiency is 12%. Output wavelength can be tuned from 2063.81 nm to 2067.20 nm by inserting a Fabry-Perot etalon and it contains the absorption line center of  $\text{CO}_2$  (2064.41 nm) [28], which makes it possible to be used in DIAL for the measurement of  $\text{CO}_2$  concentration [29]. The results demonstrate that the SLM Ho: YLF ring laser with double corner cubes configuration is an effective way to improve the misalignment sensitivity.

## 2. Experimental setup

The experimental setup is schematically depicted in Fig. 1. The

\* Corresponding author.

E-mail address: [juyoulun2015@163.com](mailto:juyoulun2015@163.com) (Y. Ju).

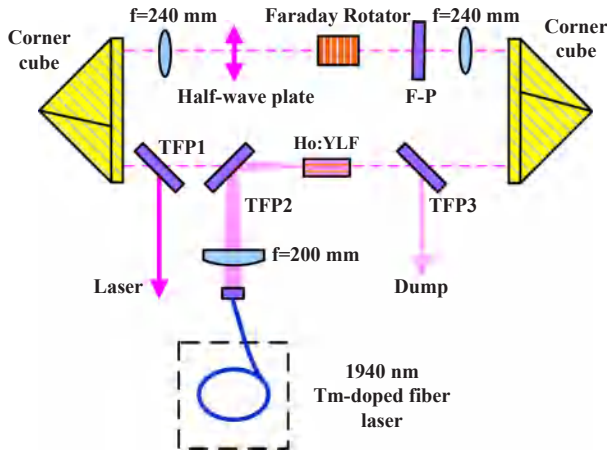


Fig. 1. Experimental setup of the SLM Ho: YLF ring laser with double corner cubes.

1940 nm Tm-doped fiber laser used for pump light is focused into an a-cut Ho: YLF crystal with spot radius of 250 μm. The gain medium of Ho: YLF is controlled at 13 °C by a TEC cooler with dopant concentrations of 0.5% and a dimension of 4 × 4 × 20 mm<sup>3</sup>, and the end faces are coated with high transmission at laser wavelength and pump wavelength. TFP1, TFP2 and TFP3 are both polarizer with high transmission for 2.05 μm p-polarized light and high reflectivity for 2.05 μm s-polarized light and 1.94 μm pump light. Polarizer TFP2 and TFP3 can be used respectively for pump light injecting and dumping, and polarizer TFP1 is the output mirror of the high spectral purity SLM lasing. The two plane convex lenses (f = 240 mm) are inserted into the resonator with the length of about 704 mm to compensate the negative lens effect of the Ho: YLF crystal. The incident planes of two corner cube prisms are high transmission at laser wavelength and pump wavelength and the reflected surfaces are both uncoated. Each of the six surface sequences will produce different output polarization which is due to the phase offsets between the six reflected paths. Output coupler transmittance can be changed through rotating half-wave plate. Faraday rotator with a polarization rotation angle of 45° is used to achieve SLM operation. A uncoated F-P etalon with the thickness of 0.3 mm is used to tune frequency.

In considering of the depolarization effect of double corner cubes resonator, the following analysis mechanism of unidirectional operation of the Ho: YLF ring laser with double corner cubes is presented with the method of optic matrix and transition matrix. Assuming that the real edges of the two corner cube prisms exist cross angle α in the plane of projection, and the light emitted by the Ho: YLF crystal is horizontal polarization. Jones matrix in anticlockwise direction and clockwise direction after a cycle can be respectively written as

$$Q_1' = F \cdot V(-\alpha) \cdot J \cdot F \cdot V(\alpha) \cdot D \cdot J_h(\theta) \cdot J \cdot E_{in} \quad (1)$$

$$Q_2' = F \cdot J \cdot F \cdot J_h(180-\theta) \cdot D \cdot V(-\alpha) \cdot J \cdot V(\alpha) \cdot E_{in} \quad (2)$$

where  $E_{in} = \langle 1, 0 \rangle$  represents the matrix of horizontal polarization light.  $V$  is rotation matrices, and  $F$ , means coordinate reflection.  $J$  is the Jones matrix of corner cube prism [30].  $D$  represents Jones matrix of faraday rotator.  $J_h$  is Jones matrix of half-wave plate, and  $\theta$  is the angle between the x axis and the fast axis of the half-wave plate.

There is no faraday rotator in the cavity for the Fig. 2(a). Both polarizer TFP1 and TFP3 are output mirrors and the corresponding equivalent output mirror transmission can be obtained by the Jones matrix in anticlockwise direction and clockwise direction, respectively.

$$T = E_y^2 / (E_x^2 + E_y^2) \quad (3)$$

where  $E_x$  and  $E_y$  are positive electric field amplitudes of output light in the x and y directions.

When the cross angle is 0°, the equivalent transmission of polarizer TFP1 and TFP3 keep all the same and therefore the Ho: YLF laser is bidirectional operation. As shown in Fig. 2(b), when a faraday rotator inserted into the cavity, the equivalent transmission of polarizer TFP1 and TFP3 can reach 20% and 100% respectively at some rotation angles. Thus only anticlockwise direction laser can be produced by the TFP1. Similarly, the equivalent transmission of polarizer TFP1 and TFP3 can reach 100% and 20% respectively at some other rotation angles. At this time, only clockwise direction laser can be produced. The SLM Ho: YLF operation can be realized without the spatial hole-burning effect. Fig. 3 shows the equivalent transmission of polarizer TFP1 and TFP3 under different rotation angle of half-wave plate and cross angle of two corner cube prisms. We can know that the equivalent transmission of polarizer TFP1 and TFP3 varies periodically with the rotation angle of half-wave plate. Even when the cross angle of two corner cube prisms ranges from 0°–30°, the equivalent transmissions have great difference at some rotation angles of half-wave plate, and unidirectional operation also can be realized, as shown in Fig. 3(a) and (b). The results show that the placement error of two corner cube prisms is allowed in the experiment.

### 3. Experimental results and discussion

Output characteristics of the free-running Ho: YLF ring laser (without a faraday rotator inserted) with double corner cubes is firstly investigated. With the rotation of the half-wave plate, the output power of the two directions is almost the same and the maximum total power points are observed four times in a cycle which is in accordance with the results in Fig. 2(b).

The detuning of the corner cube prism consisting of tilt angle and translation distance is an important physical quantity that affects the output power of the Ho:YLF ring laser. The tilt angle of the corner cube prism is changed by an adjustable mirror mount and the vertex of the corner cube prism will also move slightly with the change of tilt angle. From Fig. 4(a), we can know that with the increase of the tilt angle, the highest total power of 740 mW with the pump power of 9.8 W decreases gradually. When the tilt angle is about 1.5°, output power drops by 6%. Output power drops by 30% and the corresponding angle is about 11.8°. The results show that the laser power is less sensitive to the change of the tilt angle. The effect of translation distance of the corner cube prism on the output power of the Ho:YLF ring laser is also measured experimentally. A high precision translation stage is fixed to the corner cube prism and the translation direction of corner cube prism is perpendicular to the optical axis. As shown in Fig. 4(b), output power drops by 18% and the corresponding translation distance is about 0.2 mm. When the translation distance is about 0.35 mm, output power drops by 80%. The output power with slow decreasing is also observed when the tilt angle of polarizer and two plane convex lenses are increasing from arc second grade to degrees. The results show that the anti-misalignment ability of Ho: YLF ring laser can be greatly improved by employing double corner cubes.

When a faraday rotator and half-wave plate are inserted into the cavity, unidirectional operation can be realized by rotating the half-wave plate. Exactly as the numerical simulation, both polarizer TFP1 and TFP3 can act as output mirror of the unidirectional operation laser at different rotation angle of the half-wave plate. Here, polarizer TFP1 was used as the output mirror and output laser was vertical polarization measured by Glan prism. As shown in Fig. 5, the laser operated at single-longitudinal-mode measured by the scanned Fabry-Perot interferometer with 1.5 GHz free spectral region (FSR) at 2065.71 nm. In the inset of Fig. 5, the upper curve means the piezo actuator's driving voltage and the lower lines represent the longitudinal mode of laser and the laser is running on SLM. The laser could maintain single-longitudinal-mode operation without an etalon for the reason that the loss difference between the two directions of propagation was big enough.

When an F-P etalon with the thickness of 0.3 mm inserted into the

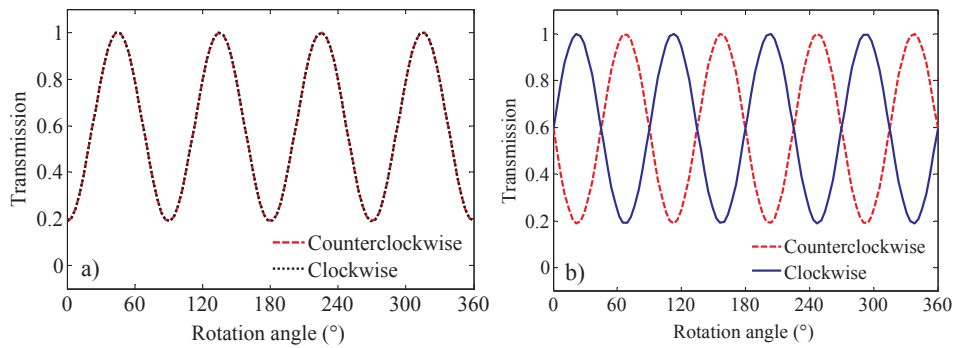


Fig. 2. Equivalent transmissions as a function of rotation angle (a) bidirectional operation (b) unidirectional operation.

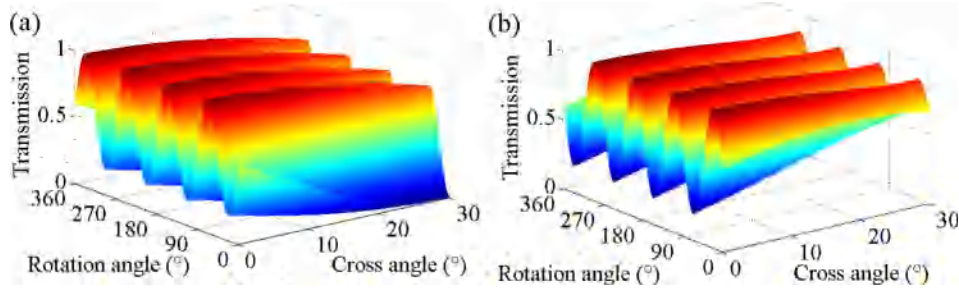


Fig. 3. Equivalent transmissions (a) polarizer TFP1 (b) polarizer TFP3.

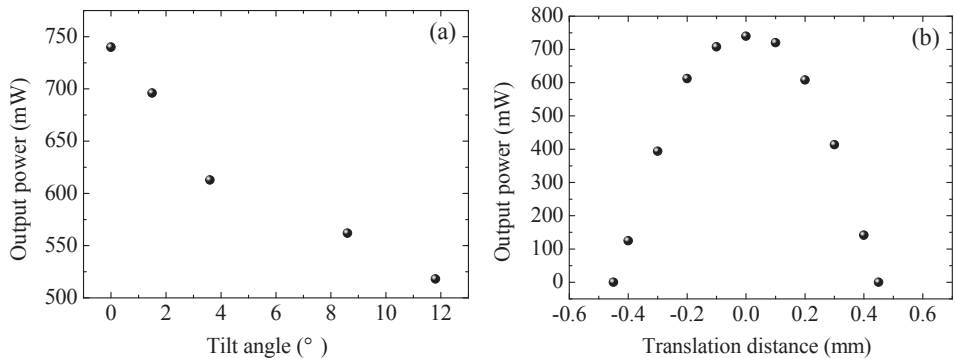


Fig. 4. Effect of the corner cube prism detuning on the laser power (a) angle detuning (b) translation detuning.

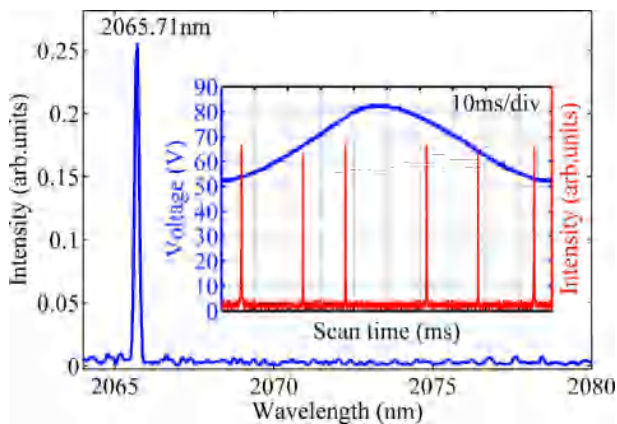


Fig. 5. Wavelength and F-P spectrum of SLM Ho: YLF ring laser with double corner cubes.

cavity, it can be known from the wavemeter (Bristol) that the wavelength of SLM Ho: YLF laser can be tuned from 2063.81 nm to 2067.20 nm and the corresponding F-P spectra shift accordingly, as

shown in Fig. 6. The F-P spectrum is measured by a F-P interferometer. The transmission peak of F-P etalon and the gain curve determine the output power and wavelength of the laser. The maximum output power is 733 mW corresponds to the laser wavelength of 2065.68 nm and the minimum output power is 628 mW, corresponding to the wavelength of 2063.81 nm. In addition, it is obviously that the method of F-P etalon is quasi-continuous tuning and the minimum tunable gap is the FSR of cavity (about 0.426 GHz). Continuous tuning can be achieved by tuning the laser cavity length, such as adding a piezoelectric ceramic transducer upon a corner cube.

As shown in Fig. 7(a), the output power of the SLM Ho: YLF ring laser with double corner cubes increases with the pump power increasing at the wavelength of 2065.68 nm. The maximum SLM output power is 733 mW under the absorbed pump power of 9.8 W and the slope efficiency is 12%. Fig. 7(b) shows the beam radius versus the distance from lens measured by knife-edge method.  $M^2$  factor of 1.21 can be achieved by fitting the measured data according to the standard Gaussian beam propagation expression and the transverse modes of the output beam can be seen in Fig. 8. The Ho: YLF ring laser with double corner cubes was running on SLM operation.

The traditional solid-state SLM lasers (such as bow-tie ring laser) generally consist of several mirrors. Once the tilt angle of a cavity

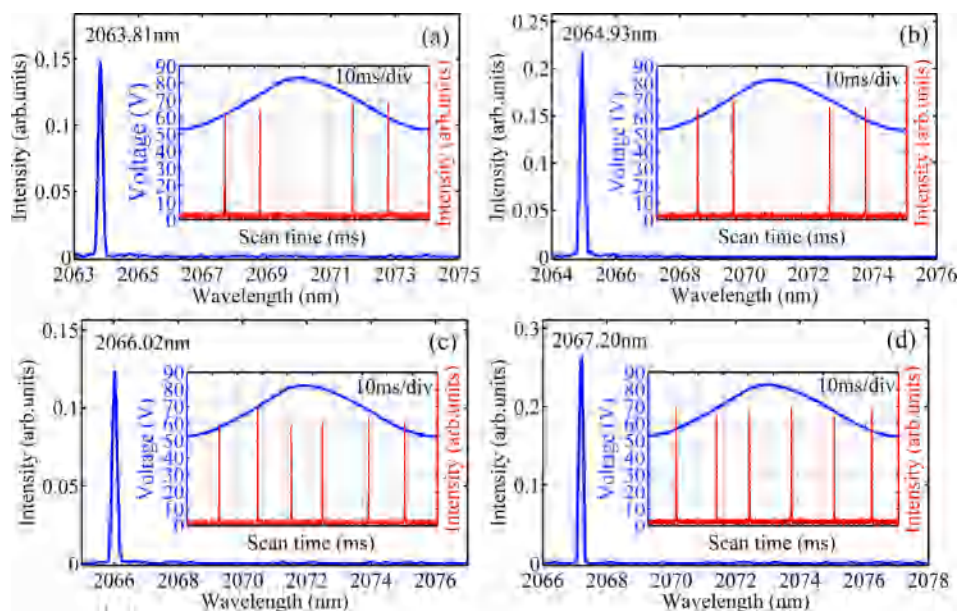


Fig. 6. Out wavelength of the SLM Ho: YLF ring laser with double corner cubes and corresponding F-P spectra.

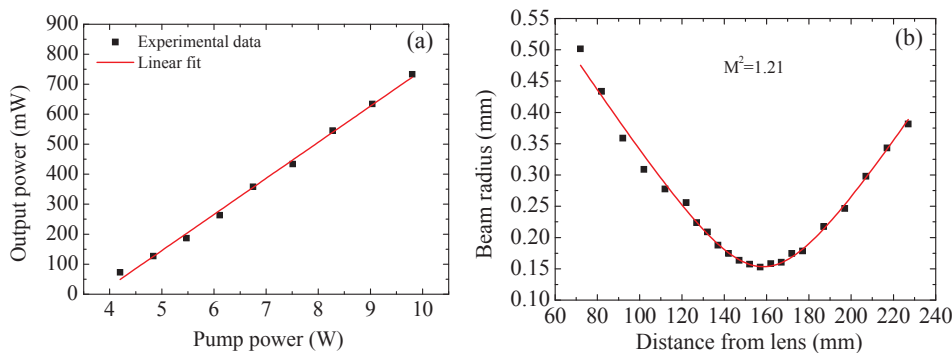


Fig. 7. Output characteristics of the SLM Ho: YLF ring laser with double corner cubes (a) output power (b) beam quality.

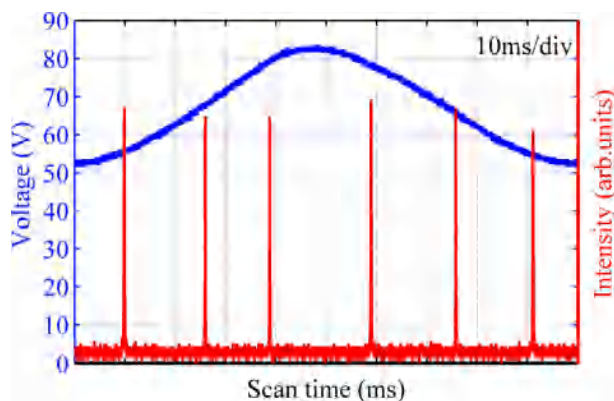


Fig. 8. F-P spectra of the SLM Ho: YLF ring laser with double corner cubes.

mirror reaches arc second grade, several longitudinal modes will generate. In this experiment, we found that the tilt angle of the mirrors (including corner cube prisms, polarizer and plane convex lenses) were far greater than arc second grade, Ho: YLF ring laser was still operating on SLM. When parallel shift distance of the corner cube reached about  $\pm 0.15$  mm, multimode oscillation was observed, and it can be overcome in the corner cube position design.

#### 4. Conclusion

In this letter, a novel SLM Ho: YLF ring laser with double corner cubes is presented for potential applications of atmospheric CO<sub>2</sub> measurement. The principle of the SLM Ho: YLF ring laser with double corner cubes is firstly analyzed with the method of optic matrix and transition matrix. The highest SLM power at 2065.68 nm is 733 mW with the slope efficiency of 12%. The tunable range is about 238 GHz with M<sup>2</sup> factor of 1.21. The results demonstrate that the introduction of double corner cubes is a potential way to improve the misalignment sensitivity of the SLM Ho: YLF ring laser.

#### Conflict of interest

We declare that we have no conflict of interest.

#### Acknowledgements

This work was supported by National Natural Science Foundation of China (No. 61405047).

#### References

- [1] T.Y. Dai, Y.L. Ju, B.Q. Yao, Y.J. Shen, W. Wang, Y.Z. Wang, Single-frequency, Q-switched Ho: YAG laser at room temperature injection-seeded by two F-P etalons-restricted Tm: Ho: YAG laser, *Opt. Lett.* 37 (2012) 1850–1852.
- [2] C.T. Wu, Y.L. Ju, Q. Wang, Z.G. Wang, B.Q. Yao, Y.Z. Wang, Injection-seeded Tm:

- YAG laser at room temperature, *Opt. commun.* 284 (2011) 994–998.
- [3] L. Wang, C.Q. Gao, M.W. Gao, Y. Li, F.Y. Yue, L. Liu, Single-frequency and dual-wavelength Ho: YAG nonplanar ring oscillator resonantly pumped by a Tm: YLF laser, *Opt. Eng.* 53 (2014) 061603.
- [4] J. Li, S.H. Yang, C.M. Zhao, H.Y. Zhang, W. Xie, Coupled-cavity concept applied to a highly compact single-frequency laser operating in the 2  $\mu\text{m}$  spectral region, *Appl. Opt.* 50 (2011) 1329–1332.
- [5] T.Y. Dai, Y.L. Ju, X.M. Duan, Y.J. Shen, B.Q. Yao, Y.Z. Wang, 2130.7 nm, Single-frequency Q-switched operation of Tm, Ho: YAlO<sub>3</sub> laser injection-seeded by a microchip Tm, Ho: YAlO<sub>3</sub> laser, *Appl. Phys. Express* 5 (2012) 082702.
- [6] T.Y. Dai, Y.L. Ju, X.M. Duan, W. Liu, B.Q. Yao, Y.Z. Wang, Single-frequency, injection-seeded Q-switched operation of a resonantly pumped Ho: YAlO<sub>3</sub> laser at 2,118 nm, *Appl. Phys. B* 111 (2013) 89–92.
- [7] B.Q. Yao, F. Chen, C.H. Zhang, Q. Wang, C.T. Wu, X.M. Duan, Room temperature single-frequency output from a diode-pumped Tm, Ho: YAP laser, *Opt. Lett.* 36 (2011) 1554–1556.
- [8] X.L. Zhang, S. Zhang, N.N. Xiao, J.H. Cui, J.Q. Zhao, L. Li, Diode-end-pumped continuously tunable single frequency Tm, Ho: LLF laser at 2.06  $\mu\text{m}$ , *Appl. Opt.* 53 (2014) 1488–1492.
- [9] F. Gibert, P.H. Flamant, D. Bruneau, C. Loth, Two-micrometer heterodyne differential absorption lidar measurements of the atmospheric CO<sub>2</sub> mixing ratio in the boundary layer, *Appl. Opt.* 45 (2006) 4448–4458.
- [10] C. Nagasawa, T. Suzuki, H. Nakajima, H. Hara, K. Mizutani, Characteristics of single longitudinal mode oscillation of the 2  $\mu\text{m}$  Tm, Ho: YLF microchip laser, *Opt. Commun.* 200 (2001) 315–319.
- [11] L. Wang, C.Q. Gao, M.W. Gao, Y. Li, Resonantly pumped monolithic nonplanar Ho: YAG ring laser with high-power single-frequency laser output at 2122 nm, *Chin. Phys. Lett.* 31 (2014) 074204.
- [12] T.F. Refaat, U.N. Singh, J. Yu, M. Petros, R. Remus, S. Ismail, Double-pulse 2- $\mu\text{m}$  integrated path differential absorption lidar airborne validation for atmospheric carbon dioxide measurement, *Appl. Opt.* 55 (2016) 4232–4246.
- [13] S. Ishii, K. Mizutani, H. Fukuoka, T. Ishikawa, B. Philippe, H. Iwai, T. Aoki, T. Itabe, A. Sato, K. Asai, Coherent 2  $\mu\text{m}$  differential absorption and wind lidar with conductively cooled laser and two-axis scanning device, *Appl. Opt.* 49 (2010) 1809–1817.
- [14] F. Gibert, D. Edouart, C. Cénac, F.L. Mounier, 2- $\mu\text{m}$  High Power Multiple-frequency Single Mode Q-switched Ho: YLF Laser for DIAL Applications, *Appl. Phys. B* 116 (2014) 967–976.
- [15] T.F. Refaat, U.N. Singh, J. Yu, M. Petros, S. Ismail, M.J. Kavaya, K.J. Davis, Evaluation of an airborne triple-pulsed 2  $\mu\text{m}$  IPDA lidar for simultaneous and independent atmospheric water vapor and carbon dioxide measurements, *Appl. Opt.* 54 (2015) 1387–1398.
- [16] J.R. Yu, A. Braud, M. Petros, 600-mJ, double-pulse 2- $\mu\text{m}$  laser, *Opt. Lett.* 28 (2003) 540–542.
- [17] J. Wu, Y.L. Ju, T.Y. Dai, B.Q. Yao, Y.Z. Wang, 1.5 W high efficiency and tunable single-longitudinal-mode Ho: YLF ring laser based on Faraday effect, *Opt. Express* 25 (2017) 27671–27677.
- [18] J. Wu, Y.L. Ju, T.Y. Dai, W. Liu, B.Q. Yao, Y.Z. Wang, A Linearly Polarized Ho: YAG Laser at 2.09  $\mu\text{m}$  with Corner Cube Cavity Pumped by Tm: YLF Laser, *Chin. Phys. Lett.* 32 (2015) 074207.
- [19] J. Liu, R.M.A. Azzam, Polarization properties of corner-cube retroreflectors: theory and experiment, *Appl. Opt.* 36 (1997) 1553–1559.
- [20] K.Y. Wu, S.H. Yang, C.M. Zhao, G.H. Wei, Single-frequency Nd:YAG ring lasers with corner cube prism, *Chin. Phys. Lett.* 17 (2000) 728–730.
- [21] Y.F. Ma, H.J. Li, J.P. Lin, X. Yu, Greatly improved stability of passively Q-switched Ce: Nd: YAG laser by using corner cube prism, *Laser Phys.* 20 (2010) 1802–1805.
- [22] Y. Cheng, X. Liu, Q. Wan, M.Z. Zhen, C.W. Mi, C.Y. Tan, S.F. Wei, X. Chen, Mutual injection phase locking coherent combination of solid-state lasers based on corner cube, *Opt. Lett.* 38 (2013) 5150–5152.
- [23] J. Wu, Y.L. Ju, T.Y. Dai, Z.G. Zhang, B.Q. Yao, Y.Z. Wang, Development of a Single-Longitudinal-Mode Ho: YAG Laser Based on Corner Cube, *Chin. Phys. Lett.* 33 (2016) 044203.
- [24] W. Koen, C. Bollig, H. Strauss, M. Schellhorn, C. Jacobs, M.J.D. Esser, Compact fibre-laser-pumped Ho: YLF oscillator-amplifier system, *Appl. Phys. B* 99 (2010) 101–106.
- [25] H.J. Strauss, W. Koen, C. Bollig, M.J.D. Esser, C. Jacobs, O.J.P. Collett, D.R. Preussler, Ho: YLF & Ho: LuLF slab amplifier system delivering 200 mJ, 2  $\mu\text{m}$  single-frequency pulses, *Opt. Express* 19 (2011) 13974–13979.
- [26] A.D. Lieto, A. Gambetta, D. Gatti, M. Marangoni, A.D. Lieto, M. Tonelli, G. Galzerano, P. Laporta, 1.6-W self-referenced frequency comb at 2.06  $\mu\text{m}$  using a Ho: YLF multipass amplifier, *Opt. Lett.* 36 (2011) 2299–2301.
- [27] H.J. Strauss, D. Preussler, M.J. Esser, W. Koen, C. Jacobs, O.J.P. Collett, C. Bollig, 330 mJ single-frequency Ho: YLF slab amplifier, *Opt. Lett.* 38 (2013) 1022–1024.
- [28] F. Gibert, L. Joly, I. Xuéref-Rémy, M. Schmidt, A. Royer, P.H. Flamant, M. Ramonet, B. Parvitte, G. Durry, V. Zéninari, Inter-comparison of 2  $\mu\text{m}$  Heterodyne Differential Absorption Lidar, Laser Diode Spectrometer, LICOR NDIR analyzer and flask measurements of near-ground atmospheric CO<sub>2</sub> mixing ratio, *Spectrochim. Acta A* 71 (2009) 1914–1921.
- [29] F. Gibert, D. Edouart, C. Cénac, F. Le Mounier, A. Dumas, 2- $\mu\text{m}$  Ho emitter-based coherent DIAL for CO<sub>2</sub> profiling in the atmosphere, *Opt. Lett.* 40 (2015) 3093–3096.
- [30] T.W. Murphy Jr., S.D. Goodrow, Polarization and far-field diffraction patterns of total internal reflection corner cubes, *Appl. Opt.* 52 (2013) 117–126.